


Article

Aloin Suppresses Lipopolysaccharide-Induced Inflammatory Response and Apoptosis by Inhibiting the Activation of NF- κ B

Xuan Luo ¹, Haowei Zhang ² , Xiduan Wei ¹, Mengjuan Shi ¹, Ping Fan ¹, Weidong Xie ^{1,2}, Yaou Zhang ^{1,2} and Naihan Xu ^{1,2,*}

¹ Key Lab in Healthy Science and Technology, Division of Life Science, Graduate School at Shenzhen, Tsinghua University, Shenzhen 518055, China; lxuan0721@163.com (X.L.); weixiduan@126.com (X.W.); 18700809087@163.com (M.S.); pingf01@126.com (P.F.); xiewd@tsinghua.edu.cn (W.X.); zhangyo@sz.tsinghua.edu.cn (Y.Z.)

² Open FIESTA Center, Tsinghua University, Shenzhen 518055, China; zhwjack@hotmail.com

* Correspondence: xu.naihan@sz.tsinghua.edu.cn; Tel.: +86-755-26036357

Received: 19 January 2018; Accepted: 17 February 2018; Published: 26 February 2018

Abstract: Numerous herbal-derived natural products are excellent anti-inflammatory agents. Several studies have reported that aloin, the major anthraquinone glycoside obtained from the *Aloe* species, exhibits anti-inflammatory activity. However, the molecular mechanism of this activity is not well understood. In this report, we found that aloin suppresses lipopolysaccharide-induced pro-inflammatory cytokine secretion and nitric oxide production, and downregulates the expression of tumor necrosis factor alpha (TNF- α), interleukin 6 (IL-6), inducible nitric oxide synthase (iNOS), and cyclooxygenase-2 (COX-2). Aloin inhibits the phosphorylation and acetylation of the NF- κ B p65 subunit by suppressing the upstream kinases p38 and Msk1, preventing LPS-induced p65 translocation to the nucleus. We have also shown that aloin inhibits LPS-induced caspase-3 activation and apoptotic cell death. Collectively, these findings suggest that aloin effectively suppresses the inflammatory response, primarily through the inhibition of NF- κ B signaling.

Keywords: inflammation; aloin; NF- κ B; macrophages; apoptosis

1. Introduction

In response to infection or tissue injury, immune cells initiate signaling cascades that trigger the release of various pro-inflammatory cytokines to combat tissue injury or pathogen invasion. Macrophages play important roles in the initiation, maintenance, and resolution of inflammation. Macrophage dysfunction can cause a variety of human inflammatory disorders, such as microbial infection, sepsis-related multiple organ failure, tumorigenesis, cardiovascular and metabolic diseases, and autoimmune diseases.

The transcription factor NF- κ B plays a vital role in inflammatory and immune responses. NF- κ B is highly activated at sites of inflammation in many diseases, and can induce the transcription of pro-inflammatory cytokines and chemokines, as well as various target genes, including inducible nitric oxide synthase (iNOS) and cyclooxygenase-2 (COX-2) [1–3]. The feasibility and efficacy of specific inhibition of NF- κ B activity has been shown in several animal models of inflammatory disease [4–6]. The NF- κ B complex contains sites for post-translational modifications, which are important for activation and crosstalk with other signaling pathways [1,7,8]. The phosphorylation and acetylation of the p65/RelA subunit are crucial post-translational modifications that are required for NF- κ B activation. The phosphorylation of p65 by PKAc, MSK1, RSK1, IKK α / β , and PKC ζ enhances its interaction with the co-activator p300/CBP, and stimulates the activity of NF- κ B [9,10]. The p65

subunit of NF- κ B is also known to be activated in an acetylation-dependent manner in response to inflammatory stimuli. The site-specific acetylation of p65 differentially regulates the distinct biological activities of the NF- κ B transcription factor complex [11]. For instance, the acetylation of lysine 310 is indispensable for the full transcriptional activity of p65. However, lysine 122 and 123 acetylation regulate the I κ B α -mediated attenuation of NF- κ B transcriptional activity, which is an important process that restores the latent state in post-induced cells [11–13].

Natural products are important sources of drugs against a variety of diseases, such as cancer and infectious diseases. Many natural products that have in anti-cancer and anti-inflammatory activity have been shown to inhibit NF- κ B. Aloin, which is also known as barbaloin, is the major anthraquinone glycoside obtained from the *Aloe* species. Several lines of evidence demonstrate that aloin exhibits anti-oxidative and anti-inflammatory activities in rats and murine macrophages [14–18]. Aloin also shows a pronounced anti-proliferative effect, the treatment of aloin-induced cell cycle arrest, and apoptotic cell death in several human cancer cell lines [19–22]. Moreover, a cell line-derived xenograft mouse model indicates that aloin inhibits tumor angiogenesis and growth via blocking STAT3 activation [23]. In this study, we evaluate the potential anti-inflammatory activity of aloin in RAW 264.7 cells. We show that aloin protects macrophages from a lipopolysaccharide (LPS)-induced inflammatory response by inhibiting the NF- κ B signaling pathway. Aloin blocks the phosphorylation, acetylation, and nuclear translocation of the NF- κ B p65 subunit. Aloin also downregulates stress-related gene expression, and protects macrophages from an LPS-induced inflammatory response and apoptotic cell death.

2. Results

2.1. Effects of Aloin on Cell Viability in Macrophages

To evaluate the cytotoxicity of aloin, RAW 264.7 cells were incubated with different concentrations of aloin for 24 h, in the presence or absence of lipopolysaccharide (LPS), after which cell viability was determined by methyl thiazolyl tetrazolium (MTT) assay. High concentrations of aloin (up to 500 μ M) did not show significant cytotoxicity in RAW 264.7 cells (Figure 1A,B). Rather, the addition of LPS enhanced cell proliferation in macrophages, and aloin had no effect on LPS-induced cell proliferation when compared with the control cells (Figure 1C).

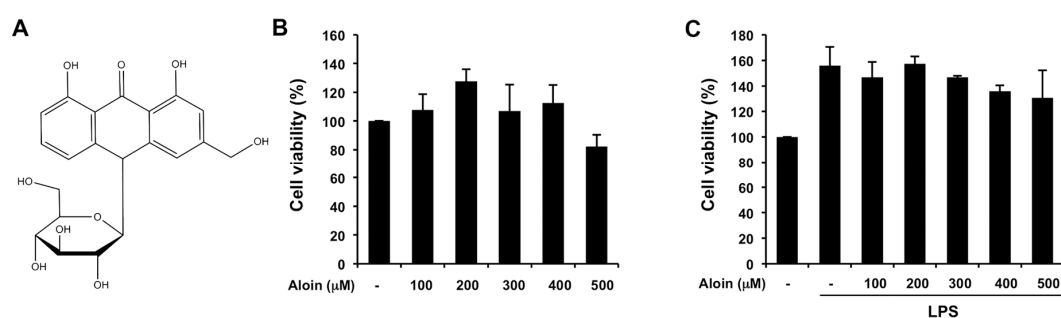


Figure 1. Aloin does not affect cell growth in murine macrophages: (A) Chemical structure of aloin; (B) RAW 264.7 cells were treated with various concentrations of aloin (100 μ M, 200 μ M, 300 μ M, 400 μ M, and 500 μ M) for 24 h. The total number of viable cells was determined by methyl thiazolyl tetrazolium (MTT) assay. Values are mean \pm SD of three independent experiments; (C) RAW 264.7 cells were treated with various concentrations of aloin and lipopolysaccharide (LPS) (100 ng/mL) for 24 h. The total number of viable cells was calculated. Values ARE mean \pm SD of three independent experiments.

2.2. Aloin Inhibits LPS-Induced IL-6 and TNF- α Expression

To investigate the effect of aloin on the LPS-induced inflammatory response, we measured the secretion of inflammatory cytokines in RAW 264.7 cells. LPS dramatically stimulated the production

of pro-inflammatory cytokines, such as tumor necrosis factor alpha (TNF- α) and interleukin 6 (IL-6), as compared with control cells. Aloin efficiently suppressed the elevated cytokine levels in LPS-treated macrophages in a dose-dependent manner (Figure 2A,B). We also investigated whether or not aloin could inhibit the LPS-induced transcription of TNF- α and IL-6 by real-time PCR. Total RNA was extracted six hours after LPS and/or aloin treatment, and aloin was found to markedly reduce LPS-induced TNF- α and IL-6 transcription (Figure 2C,D). These data indicate that aloin inhibits the LPS-induced inflammatory response in murine macrophages.

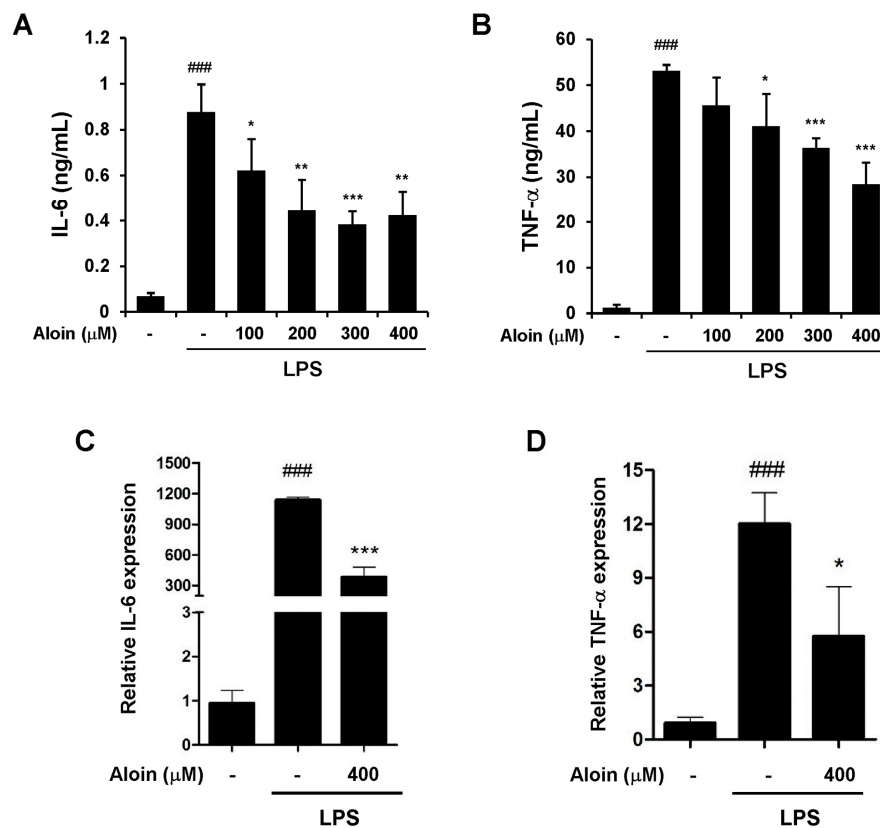


Figure 2. Aloin inhibits the LPS-induced expression of IL-6 and TNF- α RAW 264.7 cells were pre-treated with aloin for 2 h prior to LPS (100 ng/mL) stimulation. Cell-free supernatants were collected to detect (A) Interleukin 6 (IL-6) and (B) Tumor necrosis factor alpha (TNF- α) concentrations via ELISA after LPS treatment for 9 h and 24 h, respectively. The mRNA expression levels of (C) IL-6 and (D) TNF- α were determined by qPCR in RAW 264.7 cells pre-treated with aloin (400 μ M) followed by LPS (100 ng/mL) stimulation for 6 h. The data shown are the means \pm SD of three experiments. ### $p < 0.001$ is significantly different from the control. * $p < 0.05$, ** $p < 0.01$, and *** $p < 0.001$ are different from the LPS alone.

2.3. Aloin Attenuates LPS-Induced NO Production

Because nitric oxide (NO) is recognized as a mediator and regulator of inflammatory responses, we next determined the effect of aloin on NO production. As shown in Figure 3A, NO levels were dramatically increased from resting up to ~ 10 μ M following LPS treatment. The dose-dependent inhibition of NO production was observed when RAW 264.7 cells were pre-treated with different concentrations of aloin (Figure 3A).

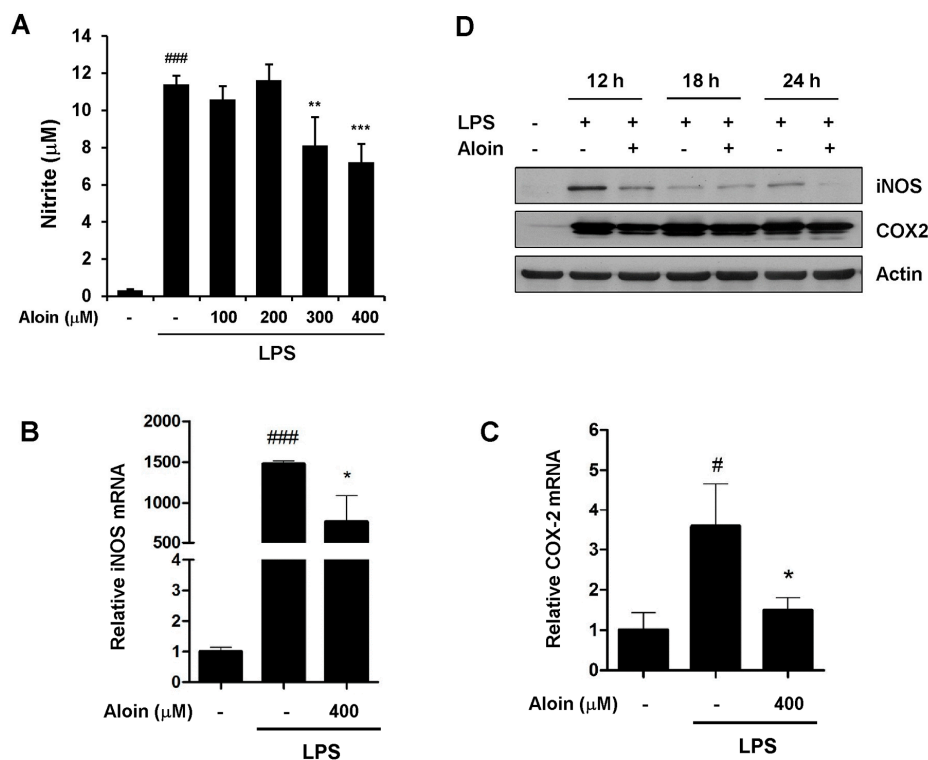


Figure 3. Aoin inhibits nitric oxide (NO) production and the expression of cyclooxygenase-2 (COX-2) and inducible nitric oxide synthase (iNOS). (A) RAW 264.7 cells were pre-treated with aoin for 2 h prior to LPS (100 ng/mL) treatment. Cell-free supernatants were collected to determine NO production using the Griess reaction after LPS treatment for 24 h. The mRNA levels of (B) iNOS and (C) COX2 were determined by qPCR; (D) RAW 264.7 cells were pre-treated with or without 400 µM aoin for 2 h, and then stimulated with LPS (100 ng/mL) for 12 h, 18 h and 24 h. Levels of iNOS and COX-2 proteins were determined by Western blotting. The results shown are the means \pm SD of three experiments. # $p < 0.05$ and ### $p < 0.001$ are significantly different from the control. * $p < 0.05$, ** $p < 0.01$, and *** $p < 0.001$ are different from the LPS alone.

2.4. Aoin Suppresses iNOS and COX-2 Expression

The inducible nitric oxide synthase (iNOS) gene is involved in the immune response and NO production. Cyclooxygenase-2 (COX-2) is rapidly induced by a variety of extracellular and intracellular stimuli, and plays a key role in promoting inflammation. We determined the effect of aoin on the expression of iNOS and COX-2 by quantitative RT-PCR and immunoblot analyses. The mRNA levels of both iNOS and COX-2 were markedly upregulated following LPS treatment (Figure 3B,C). Notably, aoin reduced LPS-induced iNOS protein expression, while it had little effect on COX-2 protein levels (Figure 3D). These results indicate that aoin suppresses LPS-induced NO production, primarily due to the aoin-mediated downregulation of iNOS.

2.5. Aoin Inhibits LPS-Induced p65 Phosphorylation and Acetylation

The LPS-induced activation of macrophages involves the Toll-like receptors. The binding of LPS to TLR4 leads to the activation of NF- κ B through the recruitment and activation of MyD88 and other adaptor proteins [24]. We examined the expression of Toll-like receptors and MyD88 in RAW 264.7 cells, and found that aoin did not affect the protein levels of TLR4, TLR7, and MyD88 in LPS-stimulated macrophages (Figure 4A).

Since NF- κ B plays an important role in the regulation of a variety of key inflammatory mediators, we sought to determine whether aoin could inhibit LPS-induced NF- κ B activation. Immunoblotting revealed that aoin reduced LPS-induced phosphorylation of p65 in a dose and time-dependent

Next, we performed an immunofluorescence assay to examine the nuclear localization of acetylated p65. First, p65 was acetylated at a very low level in the control cells, and LPS treatment dramatically increased nuclear staining of acetylated p65, while aloin markedly reduced the nuclear localization of acetylated p65 (Figure 5B,D). The nuclear translocation of p65 was also confirmed by immunostaining with a total p65 antibody. As expected, LPS treatment induced the translocation of p65 from the cytoplasm to the nucleus, and aloin prevented LPS-induced nuclear translocation in RAW 264.7 cells (Figure 5C,E).

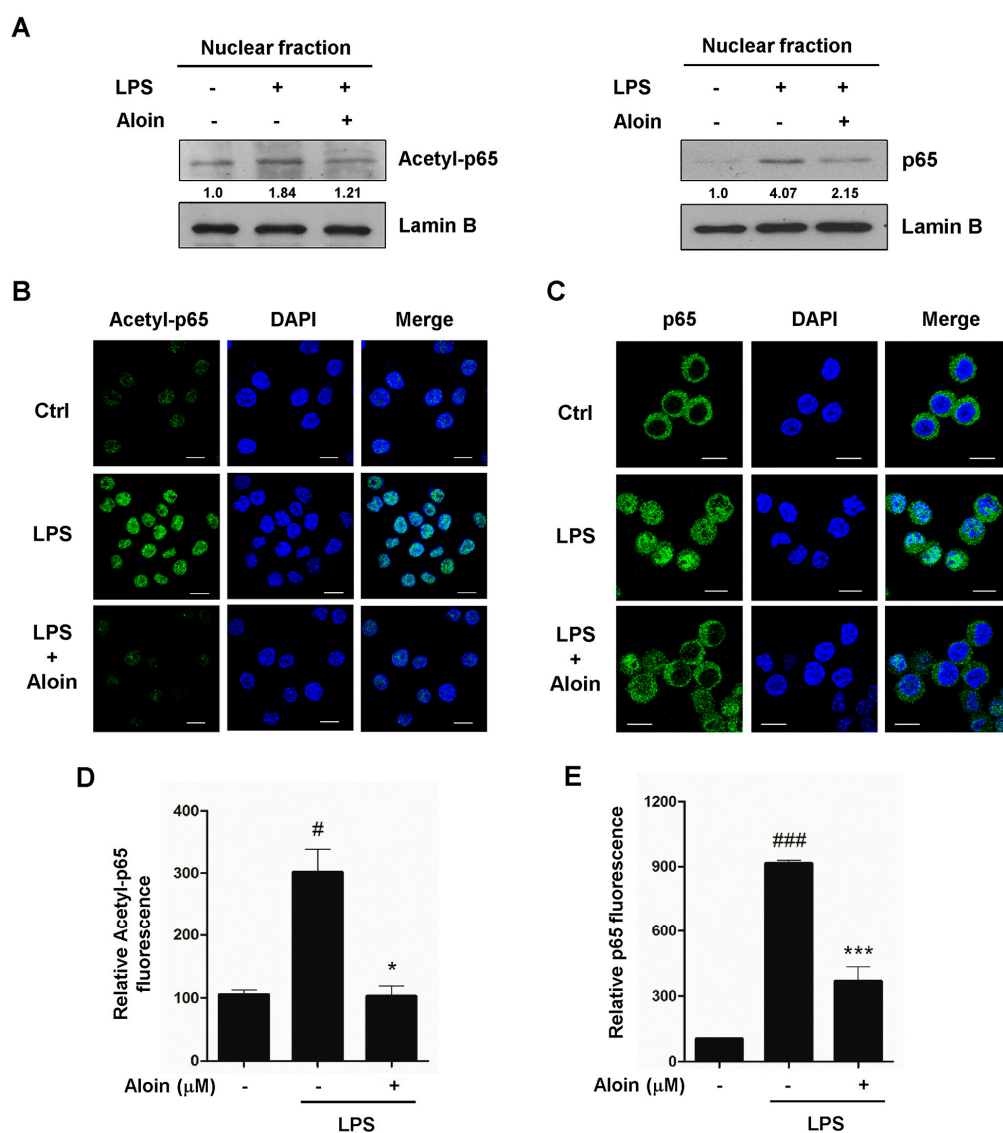


Figure 5. Aloin inhibits LPS-induced NF- κ B p65 nuclear translocation. (A) RAW 264.7 cells were pre-treated with or without aloin (400 μ M) for 2 h, and then stimulated with LPS (100 ng/mL) for 2 h. Protein levels of acetylated p65 and total p65 in the nuclear fractions were analyzed by immunoblotting. Lamin B was used as a marker for nuclear fraction. RAW 264.7 cells treated with or without aloin and LPS were fixed and immunostained with (B) acetylated p65 or (C) total p65 antibodies, and fluorescent images were captured by confocal microscopy. Scale bar, 10 μ m. At least 200 cells were counted for each sample; (D) Quantification of acetyl-p65 and (E) total p65 fluorescent intensities in RAW 264.7 cells. Data shown are the means \pm SD of three experiments. [#] $p < 0.05$ and ^{###} $p < 0.001$ are different from the control. ^{*} $p < 0.05$ and ^{***} $p < 0.001$ are different from the LPS alone.

2.7. Aloin Prevents LPS-Induced Apoptotic Cell Death

It has been reported that LPS induces apoptosis in several cell types. To evaluate the effect of aloin on LPS-induced apoptosis in macrophages, we performed annexin V/PI flow cytometry analysis to measure apoptotic cell death. Annexin-V positive cells increased with the time of LPS treatment. At 48 h after LPS administration, 62% of the cell population were apoptotic. LPS-induced apoptosis was markedly reduced by aloin treatment (Figure 6A). Immunoblotting analysis revealed that LPS caused an obvious increase in the levels of cleaved caspase-9 and caspase-3, indicating that LPS induces caspase-mediated apoptosis. Supporting the flow cytometry results, the LPS-induced cleavage of caspase-9 and caspase-3 were largely prevented by aloin (Figure 6B).

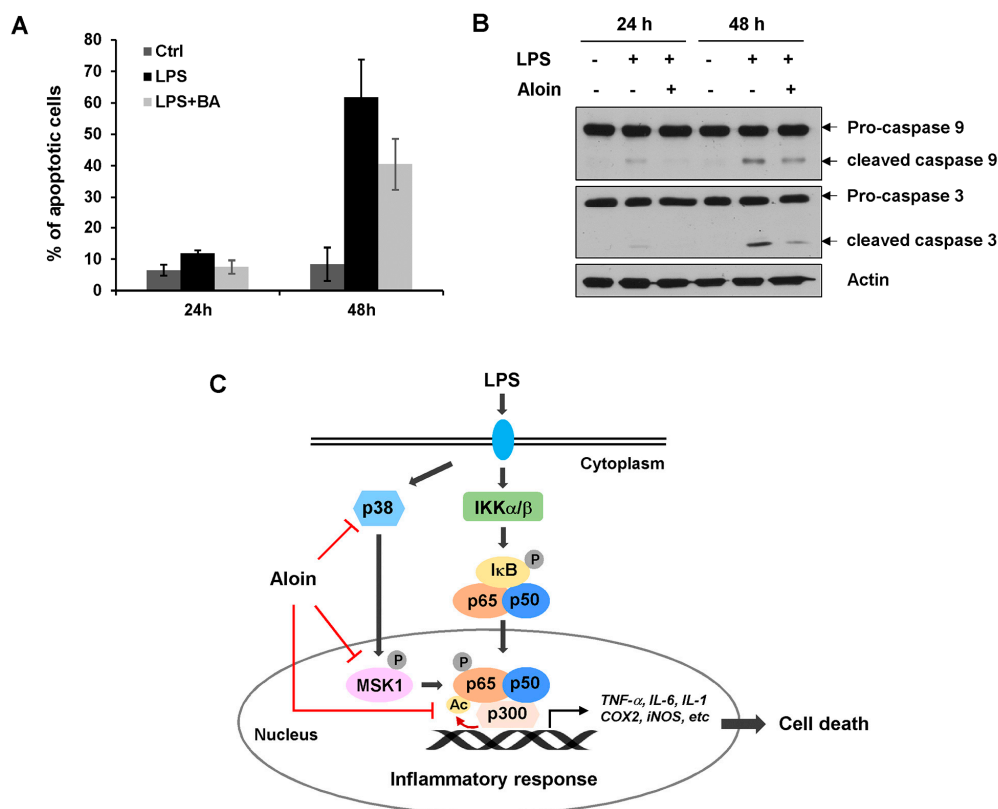


Figure 6. Aloin inhibits LPS-induced apoptotic cell death. (A) RAW 264.7 cells were pre-treated with or without aloin (400 μ M) for 2 h, and then stimulated with LPS (100 ng/mL) for 24 h or 48 h. Cells were collected and stained with Annexin V/PI, the percentage of Annexin-V positive cells was analyzed by flow cytometry analysis. Data shown are the means \pm SD of three experiments; (B) The protein expression levels of pro-caspase 9, cleaved caspase-9, pro-caspase 3, and cleaved caspase 3 were determined by immunoblotting analysis. β -actin was used as a loading control; (C) Aloin prevented the LPS-induced inflammatory response by inhibiting NF- κ B signaling. Aloin attenuated LPS-induced p65 post-translational modifications by inhibiting p38 and MSK1-mediated phosphorylation and p300-mediated acetylation. This in turn prevented p65 nuclear translocation, and downregulated NF- κ B mediated gene expression, including pro-inflammatory cytokines, and genes involved in apoptosis.

3. Discussion

Although aloin is known to have anti-inflammatory and anti-oxidative activities, the molecular basis of the anti-inflammatory effects of aloin is still unclear. In this study, we demonstrate that aloin, a natural product extracted from the *Aloe* species, is an effective anti-inflammatory agent. Aloin inhibits the LPS-induced expression and secretion of the pro-inflammatory cytokines IL-6 and TNF- α . Aloin blocks the phosphorylation, acetylation, and nuclear translocation of the NF- κ B

p65 subunit. Aloin also inhibits NO production, and downregulates stress-related gene expression. These data indicate that aloin induced anti-inflammatory activity is mediated through the inhibition of NF- κ B signaling (Figure 6C).

The phosphorylation and acetylation of p65 are critical to NF- κ B-dependent activation. LPS can activate the I κ B kinase (IKK) enzyme complex, which phosphorylates I κ B proteins. The phosphorylation of I κ B leads to its ubiquitination and degradation, releasing NF- κ B/p65 complexes. NF- κ B/p65 complexes are further activated by post-translational modifications and translocate to the nucleus [9,25,26]. We examined the upstream kinases that control p65 phosphorylation. We found that aloin inhibits the LPS-induced phosphorylation of p38 and Msk1. The p38 MAPK is crucial for LPS-induced cytokine gene expression. p38 induces the phosphorylation of histone H3, and increases DNA accessibility for NF- κ B binding at specific promoters. p38 also phosphorylates and activates Msk1, which increases transcription through the phosphorylation of p65 at serine 276. p65 Ser 276 phosphorylation promotes its own interaction with the cofactors CREB/p300, which in turn acetylates p65 itself, as well as histones at NF- κ B-bound promoters [27–29]. We also found that aloin suppressed LPS-induced p65 acetylation, and markedly reduced the nuclear translocation of p65 in LPS-stimulated macrophages. Thus, our study has uncovered a feasible mechanism in which aloin suppresses p65 post-translational modifications and nuclear translocation, and consequently attenuates the level of NF- κ B-dependent transcription and the inflammatory response.

Nitric oxide plays an important role in mediating many aspects of inflammatory responses. iNOS is one of the three enzymes that catalyze the production of NO from L-arginine [30]. It is an important factor in clearing parasites and bacterial infections. The level of NO produced by iNOS is predominantly regulated at the transcriptional level. LPS, cytokines, and oxidative stress have been shown to induce iNOS expression through the activation of NF- κ B [31,32]. COX-2 plays a key role in the inflammatory response. A variety of extracellular and intracellular stimuli, including LPS, rapidly induce COX-2 expression [33]. NF- κ B has been shown to control the induction of COX-2 transcription [34,35]. Here, we demonstrated that aloin markedly suppressed the transcription of iNOS and COX2. Aloin also decreased the level of LPS-induced NO production in RAW 264.7 cells in a dose-dependent manner. Since NF- κ B plays a pivotal role in regulating the expression of *iNOS* and *COX-2*, we conclude that aloin inhibits LPS-induced inflammatory gene expression by suppressing NF- κ B transcriptional activity.

Several studies have shown that LPS induces apoptosis in different cell types, including macrophages [36–39]. Apoptosis has been involved in multi-organ failure during septic shock [40,41]. Multiple molecular mechanisms are involved in LPS-induced apoptosis. The deleterious effects of LPS are associated with the secretion of TNF- α and NO production. Exposure to endogenous or exogenous NO, or treatment with TNF- α , are sufficient to induce apoptosis [39,42,43]. LPS induces macrophage apoptosis via two pathways; one is through the mitochondrial apoptotic cascade leading to caspase-3 activation, while the other is mediated by death receptor and caspase-8 activation [36,44,45]. Since aloin efficiently inhibits the LPS-induced inflammatory response, we investigated whether aloin played a protective effect on LPS-induced apoptosis. Both flow cytometry and immunoblotting revealed that aloin remarkably reduced the number of Annexin-V positive cells and caspase-3 cleavage, indicating that aloin has anti-apoptotic activity against LPS-induced cell death in murine macrophages. Collectively, the results of this study suggest that aloin is an effective anti-inflammatory and anti-apoptotic agent, and acts primarily through the inhibition of the NF- κ B signaling pathway.

4. Materials and Methods

4.1. Cell Culture and Reagents

RAW 264.7 cells (murine macrophage cell line) were purchased from the Cell Library of Chinese Academy of Sciences. Cells were cultured in Dulbecco modified Eagle medium (Invitrogen,

Thermofisher Scientific, Waltham, MA, USA), and supplemented with 10% fetal bovine serum (Thermofisher Scientific, Waltham, MA, USA) in a 5% CO₂-humidified incubator at 37 °C.

Aloin ($\geq 97\%$) was purchased from Shanghai Aladdin Biochemical Technology Co., Ltd. (Shanghai, China). Dimethyl sulfoxide (DMSO), lipopolysaccharide (LPS, from *Escherichia coli*) and methyl thiazolyl tetrazolium (MTT) were purchased from Sigma Chemical Co. (St. Louis, MO, USA). Aloin was dissolved in DMSO. Mouse TNF- α enzyme-linked immunosorbent assay (ELISA) and IL-6 ELISA kits were purchased from Dakewe Biotech Co., Ltd. (Shenzhen, China). The Griess reagent was purchased from the Beyotime Institute of Biotechnology (Shanghai, China). The nucleoprotein extraction kit was obtained from Sangon Biotechnology (Shanghai, China). The antibodies against iNOS, COX-2, phosphor-I κ B- α (Ser32), phosphor-IKK α / β (Ser176/180), phosphor-GSK-3 β (Ser9), phosphor-Msk1 (Thr581), p38, phosphor-p38 MAPK (Thr180/Tyr182), NF- κ B p65, phosphor-NF- κ B p65 (Ser536), Acetyl-p65 (Lys310), HDAC1, and β -actin were purchased from Cell Signaling Technology (Danvers, MA, USA).

4.2. Cell Viability Assay

Cell viability was evaluated using a MTT assay. RAW 264.7 cells were seeded into 96-well plates at a density of 7×10^3 cells per well, and maintained at 37 °C for 24 h. The cells were exposed to various concentrations of aloin (100 μ M, 200 μ M, 300 μ M, 400 μ M, and 500 μ M) and stimulated with LPS (100 ng/mL) for 24 h. After 24 h of incubation, the MTT (5 mg/mL) solution was added to each well, and incubated for another 4 h. Then, 100 μ L of DMSO was added to each well to dissolve the formazan crystals that formed, and the absorbance of the solution was measured at 490 nm. Cell viability was determined from the absorbance value, and compared with that of the untreated control group. All of the experiments were performed in triplicate.

4.3. Quantitative Real-Time PCR

Cells were seeded in six-well plates, treated with or without aloin for 2 h, and then stimulated with LPS (100 ng/mL) for 24 h. Total RNA was extracted and reverse transcribed, as previously described [46]. The expression of *iNOS*, *COX-2*, *TNF- α* , and *IL-6* mRNA was normalized to β -actin. The following primers were used for PCR analysis: *iNOS* forward 5'-GTTCTCAGCCCAACAATACAAGA-3', *iNOS* reverse 5'-GTGGACGGTTCGATGTCAC-3'; *COX-2* forward 5'-CCCCATTAGCAGCCAGTT-3', *COX-2* reverse 5'-CATTCCCCACGGTTTTGA-3'; *TNF- α* forward 5'-GGAACACGTCGTGGGATAATG-3', *TNF- α* reverse 5'-GGCAGACTTTGGATGCTTCTT-3'; *IL-6* forward 5'-GGCGGATCGGATGTTGTGAT-3', *IL-6* reverse 5'-GGACCCAGACAATCGGTTG-3'; β -actin forward 5'-TCGTGCGTGACATCAAAGA-3', β -actin reverse 5'-CATACCCAAGAAGGAAGGCT-3'.

4.4. Nitric Oxide Measurement

Cells were plated in 24-well plates and pre-treated with different concentrations of aloin (100 μ M, 200 μ M, 300 μ M, and 400 μ M) for 2 h, followed by treatment with LPS (100 ng/mL) for another 24 h. Cell-free supernatants were collected for the determination of NO content using a commercially available kit based on the Griess reaction (Beyotime).

4.5. Cytokine Measurement

Cells were plated in 24-well plates, and pre-treated with different concentrations of aloin (100 μ M, 200 μ M, 300 μ M, and 400 μ M) for 2 h, then incubated with LPS (100 ng/mL) for different time periods. Cell-free supernatants were collected for the determination of TNF- α and IL-6 concentrations via ELISA analysis (Dakewe), according the manufacturer's protocols.

4.6. Western Blot Analysis

Cells were lysed in an ice-cold whole cell extract buffer (50mM Tris-HCl, pH 8.0, 4 M urea and 1% Triton X-100) supplemented with a protease inhibitor mixture (Roche). Cell extracts were resolved by SDS-PAGE, and transferred to a nitrocellulose membrane. Membranes were probed with primary antibodies against iNOS, COX-2, p-I κ B- α , p-IKK α / β , p-GSK3 β , p-Msk1, p38, p-p38, p65, p-p65, acetyl-p65, HDAC1, and β -actin, followed by incubation with horseradish peroxidase (HRP)-conjugated secondary antibodies (KPL). Protein bands were developed using enhanced chemiluminescence (ECL) Western Blotting Substrate (Thermo Scientific, Waltham, MA, USA).

4.7. Immunofluorescence

RAW 264.7 cells were seeded in 12-well plates, pretreated with aloein (400 μ M) for 2 h, and then stimulated with LPS (100 ng/mL) for another 2 h. Cells were fixed in freshly prepared 4% paraformaldehyde solution for 15 min, washed three times with phosphate-buffered saline (PBS), and permeabilized with 0.25% Triton X-100 for 10 min. The fixed cell preparations were blocked in 3% BSA for 1 h, and incubated with p65 (Cell Signaling Technology) or acetyl-p65 (GeneTex, Irvine, CA, USA) antibodies for 1 h at room temperature. The stained cells were washed and incubated with Alexa Fluor 488 conjugated secondary antibody (Invitrogen) for 1 h. Fluorescent images were acquired using an Olympus FV1000 confocal microscope (Tokyo, Japan).

4.8. Flow Cytometry

RAW 264.7 cells were placed in six-well plates, and treated with or without aloein (400 μ M) for 2 h prior to LPS (100 ng/mL) treatment for 24 h and 48 h. Cells were harvested and processed using the Dead Cell Apoptosis Kit with Annexin V Alexa Fluor™ 488 and propidium iodide (Invitrogen). Cells were counted by using a BD Accuri C6 Flow cytometer.

4.9. Statistical Analyses

Data are expressed as mean \pm SD of three independent experiments. Statistical analyses were performed using two-tailed student's *t*-test. Differences were considered significant if $p < 0.05$.

Acknowledgments: This work was supported by the National Natural Science Foundation of China (31571418) and the Shenzhen Science and Technology Innovation Committee (JCYJ20160226185623304).

Author Contributions: X.L., H.Z., X.W., M.S. and P.F. performed the experiments; X.L. and W.X. analyzed the data; Y.Z. and N.X. designed the experiments and supervised the project; N.X. wrote the manuscript.

Conflicts of Interest: The authors declare no conflict of interest. The funding sponsors had no role in the design of the study; in the collection, analyses, or interpretation of data; in the writing of the manuscript, and in the decision to publish the results.

References

1. Oeckinghaus, A.; Ghosh, S. The NF-kappaB Family of Transcription Factors and Its Regulation. *Cold Spring Harb. Perspect. Biol.* **2009**, *1*, a000034. [[CrossRef](#)] [[PubMed](#)]
2. Tan, A.C.; Konczak, I.; Sze, D.M.; Ramzan, I. Molecular Pathways for Cancer Chemoprevention by Dietary Phytochemicals. *Nutr. Cancer* **2011**, *63*, 495–505. [[CrossRef](#)] [[PubMed](#)]
3. Tak, P.P.; Firestein, G.S. NF-kappaB: A Key Role in Inflammatory Diseases. *J. Clin. Investig.* **2001**, *107*, 7–11. [[CrossRef](#)] [[PubMed](#)]
4. Neurath, M.F.; Pettersson, S.; Meyer zum Buschenfelde, K.H.; Strober, W. Local Administration of Antisense Phosphorothioate Oligonucleotides to the p65 Subunit of NF-kappa B Abrogates Established Experimental Colitis in Mice. *Nat. Med.* **1996**, *2*, 998–1004. [[CrossRef](#)] [[PubMed](#)]

5. Tomita, T.; Takeuchi, E.; Tomita, N.; Morishita, R.; Kaneko, M.; Yamamoto, K.; Nakase, T.; Seki, H.; Kato, K.; Kaneda, Y.; et al. Suppressed Severity of Collagen-Induced Arthritis by in Vivo Transfection of Nuclear Factor kappaB Decoy Oligodeoxynucleotides as a Gene Therapy. *Arthritis Rheumatol.* **1999**, *42*, 2532–2542. [[CrossRef](#)]
6. Gerlag, D.M.; Ransone, L.; Tak, P.P.; Han, Z.; Palanki, M.; Barbosa, M.S.; Boyle, D.; Manning, A.M.; Firestein, G.S. The Effect of a T Cell-Specific NF-kappa B Inhibitor on in Vitro Cytokine Production and Collagen-Induced Arthritis. *J. Immunol.* **2000**, *165*, 1652–1658. [[PubMed](#)]
7. Hoesel, B.; Schmid, J.A. The Complexity of NF-kappaB Signaling in Inflammation and Cancer. *Mol. Cancer* **2013**, *12*, 86. [[CrossRef](#)] [[PubMed](#)]
8. Perkins, N.D. Post-Translational Modifications Regulating the Activity and Function of the Nuclear Factor Kappa B Pathway. *Oncogene* **2006**, *25*, 6717–6730. [[CrossRef](#)] [[PubMed](#)]
9. Christian, F.; Smith, E.L.; Carmody, R.J. The Regulation of NF-kappaB Subunits by Phosphorylation. *Cells* **2016**, *5*. [[CrossRef](#)] [[PubMed](#)]
10. Zhong, H.; May, M.J.; Jimi, E.; Ghosh, S. The Phosphorylation Status of Nuclear NF-kappa B Determines its Association with CBP/p300 or HDAC-1. *Mol. Cell* **2002**, *9*, 625–636. [[CrossRef](#)]
11. Chen, L.; Fischle, W.; Verdin, E.; Greene, W.C. Duration of Nuclear NF-kappaB Action Regulated by Reversible Acetylation. *Science* **2001**, *293*, 1653–1657. [[CrossRef](#)] [[PubMed](#)]
12. Kiernan, R.; Bres, V.; Ng, R.W.; Coudart, M.P.; El Messaoudi, S.; Sardet, C.; Jin, D.Y.; Emiliani, S.; Benkirane, M. Post-Activation Turn-Off of NF-kappaB-Dependent Transcription is Regulated by Acetylation of p65. *J. Biol. Chem.* **2003**, *278*, 2758–2766. [[CrossRef](#)] [[PubMed](#)]
13. Chen, L.F.; Mu, Y.; Greene, W.C. Acetylation of RelA at Discrete Sites Regulates Distinct Nuclear Functions of NF-kappaB. *EMBO J.* **2002**, *21*, 6539–6548. [[CrossRef](#)] [[PubMed](#)]
14. Beppu, H.; Koike, T.; Shimpo, K.; Chihara, T.; Hoshino, M.; Ida, C.; Kuzuya, H. Radical-Scavenging Effects of Aloe Arborescens Miller on Prevention of Pancreatic islet B-cell Destruction in Rats. *J. Ethnopharmacol.* **2003**, *89*, 37–45. [[CrossRef](#)]
15. Park, M.Y.; Kwon, H.J.; Sung, M.K. Dietary aloin, Aloesin, or Aloe-Gel Exerts anti-Inflammatory Activity in a Rat Colitis model. *Life Sci.* **2011**, *88*, 486–492. [[CrossRef](#)] [[PubMed](#)]
16. Park, M.Y.; Kwon, H.J.; Sung, M.K. Evaluation of Aloin and Aloe-Emodin as Anti-Inflammatory Agents in Aloe by Using Murine Macrophages. *Biosci. Biotechnol. Biochem.* **2009**, *73*, 828–832. [[CrossRef](#)] [[PubMed](#)]
17. Silva, M.A.; Trevisan, G.; Hoffmeister, C.; Rossato, M.F.; Boligon, A.A.; Walker, C.I.; Klafke, J.Z.; Oliveira, S.M.; Silva, C.R.; Athayde, M.L.; et al. Anti-Inflammatory and Antioxidant Effects of Aloe Saponaria Haw in a Model of UVB-Induced Paw Sunburn in Rats. *J. Photochem. Photobiol. B* **2014**, *133*, 47–54. [[CrossRef](#)] [[PubMed](#)]
18. Hamiza, O.O.; Rehman, M.U.; Khan, R.; Tahir, M.; Khan, A.Q.; Lateef, A.; Sultana, S. Chemopreventive Effects of Aloin Against 1,2-Dimethylhydrazine-Induced Preneoplastic Lesions in the Colon of Wistar Rats. *Hum. Exp. Toxicol.* **2014**, *33*, 148–163. [[CrossRef](#)] [[PubMed](#)]
19. Niciforovic, A.; Adzic, M.; Spasic, S.D.; Radojic, M.B. Antitumor Effects of a Natural Anthracycline Analog (Aloin) Involve Altered Activity of Antioxidant Enzymes in HeLaS3 cells. *Cancer Biol. Ther.* **2007**, *6*, 1200–1205. [[CrossRef](#)] [[PubMed](#)]
20. Esmat, A.Y.; Tomasetto, C.; Rio, M.C. Cytotoxicity of a Natural Anthraquinone (Aloin) Against Human Breast Cancer Cell Lines with and without ErbB-2: Topoisomerase IIalpha Coamplification. *Cancer Biol. Ther.* **2006**, *5*, 97–103. [[CrossRef](#)] [[PubMed](#)]
21. Esmat, A.Y.; El-Gerzawy, S.M.; Rifaat, A. DNA Ploidy and S Phase Fraction of Breast and Ovarian Tumor Cells Treated with a Natural Anthracycline Analog (aloin). *Cancer Biol. Ther.* **2005**, *4*, 108–112. [[CrossRef](#)] [[PubMed](#)]
22. Wan, L.; Zhang, L.; Fan, K.; Wang, J. Aloin Promotes A549 Cell Apoptosis via the Reactive Oxygen Species/mitogen Activated Protein Kinase Signaling Pathway and p53 Phosphorylation. *Mol. Med. Rep.* **2017**, *16*, 5759–5768. [[CrossRef](#)] [[PubMed](#)]
23. Pan, Q.; Pan, H.; Lou, H.; Xu, Y.; Tian, L. Inhibition of the Angiogenesis and Growth of Aloin in Human Colorectal Cancer in Vitro and In Vivo. *Cancer Cell Int.* **2013**, *13*, 69. [[CrossRef](#)] [[PubMed](#)]
24. Park, H.S.; Jung, H.Y.; Park, E.Y.; Kim, J.; Lee, W.J.; Bae, Y.S. Cutting Edge: Direct Interaction of TLR4 with NAD(P)H Oxidase 4 Isozyme is Essential for Lipopolysaccharide-Induced Production of Reactive Oxygen Species and Activation of NF-kappa B. *J. Immunol.* **2004**, *173*, 3589–3593. [[CrossRef](#)] [[PubMed](#)]

25. Hayden, M.S.; Ghosh, S. Shared Principles in NF-kappaB Signaling. *Cell* **2008**, *132*, 344–362. [[CrossRef](#)] [[PubMed](#)]
26. Chen, J.; Chen, Z.J. Regulation of NF-kappaB by Ubiquitination. *Curr. Opin. Immunol.* **2013**, *25*, 4–12. [[CrossRef](#)] [[PubMed](#)]
27. Deak, M.; Clifton, A.D.; Lucocq, L.M.; Alessi, D.R. Mitogen- and Stress-Activated Protein Kinase-1 (MSK1) is Directly Activated by MAPK and SAPK2/p38, and may Mediate activation of CREB. *EMBO J.* **1998**, *17*, 4426–4441. [[CrossRef](#)] [[PubMed](#)]
28. Vermeulen, L.; De Wilde, G.; Van Damme, P.; Vanden Berghe, W.; Haegeman, G. Transcriptional Activation of the NF-kappaB p65 Subunit by Mitogen and Stress-Activated Protein Kinase-1 (MSK1). *EMBO J.* **2003**, *22*, 1313–1324. [[CrossRef](#)] [[PubMed](#)]
29. Ghosh, S.; Hayden, M.S. New Regulators of NF-kappaB in Inflammation. *Nat. Rev. Immunol.* **2008**, *8*, 837–848. [[CrossRef](#)] [[PubMed](#)]
30. Marletta, M.A. Nitric Oxide Synthase Structure and Mechanism. *J. Biol. Chem.* **1993**, *268*, 12231–12234. [[PubMed](#)]
31. Pautz, A.; Art, J.; Hahn, S.; Nowag, S.; Voss, C.; Kleinert, H. Regulation of the Expression of Inducible Nitric Oxide Synthase. *Nitric Oxide* **2010**, *23*, 75–93. [[CrossRef](#)] [[PubMed](#)]
32. Xie, Q.W.; Kashiwabara, Y.; Nathan, C. Role of Transcription Factor NF-kappa B/Rel in Induction of Nitric Oxide Synthase. *J. Biol. Chem.* **1994**, *269*, 4705–4708. [[PubMed](#)]
33. Williams, C.S.; Mann, M.; DuBois, R.N. The Role of Cyclooxygenases in Inflammation, Cancer, and Development. *Oncogene* **1999**, *18*, 7908–7916. [[CrossRef](#)] [[PubMed](#)]
34. Schmedtje, J.F., Jr.; Ji, Y.S.; Liu, W.L.; DuBois, R.N.; Runge, M.S. Hypoxia Induces Cyclooxygenase-2 via the NF-kappaB p65 Transcription Factor in Human Vascular Endothelial Cells. *J. Biol. Chem.* **1997**, *272*, 601–608. [[CrossRef](#)] [[PubMed](#)]
35. Jobin, C.; Morteau, O.; Han, D.S.; Balfour Sartor, R. Specific NF-kappaB Blockade Selectively Inhibits Tumour Necrosis Factor-Alpha-Induced COX-2 but not Constitutive COX-1 Gene Expression in HT-29 Cells. *Immunology* **1998**, *95*, 537–543. [[CrossRef](#)] [[PubMed](#)]
36. Choi, K.B.; Wong, F.; Harlan, J.M.; Chaudhary, P.M.; Hood, L.; Karsan, A. Lipopolysaccharide Mediates Endothelial Apoptosis by a FADD-Dependent Pathway. *J. Biol. Chem.* **1998**, *273*, 20185–20188. [[CrossRef](#)] [[PubMed](#)]
37. Bannerman, D.D.; Sathyamoorthy, M.; Goldblum, S.E. Bacterial Lipopolysaccharide Disrupts Endothelial Monolayer Integrity and Survival Signaling Events Through Caspase Cleavage of Adherens Junction Proteins. *J. Biol. Chem.* **1998**, *273*, 35371–35380. [[CrossRef](#)] [[PubMed](#)]
38. Kato, Y.; Morikawa, A.; Sugiyama, T.; Koide, N.; Jiang, G.Z.; Lwin, T.; Yoshida, T.; Yokochi, T. Augmentation of Lipopolysaccharide-Induced Thymocyte Apoptosis by Interferon-Gamma. *Cell Immunol.* **1997**, *177*, 103–108. [[CrossRef](#)] [[PubMed](#)]
39. Xaus, J.; Comalada, M.; Valledor, A.F.; Lloberas, J.; Lopez-Soriano, F.; Argiles, J.M.; Bogdan, C.; Celada, A. LPS Induces Apoptosis in Macrophages mostly through the Autocrine Production of TNF-alpha. *Blood* **2000**, *95*, 3823–3831. [[PubMed](#)]
40. Parrillo, J.E. Pathogenetic Mechanisms of Septic Shock. *N. Engl. J. Med.* **1993**, *328*, 1471–1477. [[CrossRef](#)] [[PubMed](#)]
41. Parker, M.M.; Shelhamer, J.H.; Natanson, C.; Alling, D.W.; Parrillo, J.E. Serial Cardiovascular Variables in Survivors and Nonsurvivors of Human Septic Shock: Heart Rate as an early Predictor of Prognosis. *Crit. Care Med.* **1987**, *15*, 923–929. [[CrossRef](#)] [[PubMed](#)]
42. Albina, J.E.; Cui, S.; Mateo, R.B.; Reichner, J.S. Nitric Oxide-Mediated Apoptosis in Murine Peritoneal Macrophages. *J. Immunol.* **1993**, *150*, 5080–5085. [[PubMed](#)]
43. Sarih, M.; Souvannavong, V.; Adam, A. Nitric Oxide Synthase Induces Macrophage Death by Apoptosis. *Biochem. Biophys. Res. Commun.* **1993**, *191*, 503–508. [[CrossRef](#)] [[PubMed](#)]
44. Suzuki, T.; Kobayashi, M.; Isatsu, K.; Nishihara, T.; Aiuchi, T.; Nakaya, K.; Hasegawa, K. Mechanisms Involved in Apoptosis of Human Macrophages Induced by Lipopolysaccharide from *Actinobacillus Actinomycetemcomitans* in the Presence of Cycloheximide. *Infect. Immun.* **2004**, *72*, 1856–1865. [[CrossRef](#)] [[PubMed](#)]

45. Kuwabara, T.; Imajoh-Ohmi, S. LPS-Induced Apoptosis is Dependent upon Mitochondrial Dysfunction. *Apoptosis* **2004**, *9*, 467–474. [[CrossRef](#)] [[PubMed](#)]
46. Cheng, M.; Liu, L.; Lao, Y.; Liao, W.; Liao, M.; Luo, X.; Wu, J.; Xie, W.; Zhang, Y.; Xu, N. MicroRNA-181a Suppresses Parkin-Mediated Mitophagy and Sensitizes Neuroblastoma Cells to Mitochondrial Uncoupler-Induced Apoptosis. *Oncotarget* **2016**, *7*, 42274–42287. [[CrossRef](#)] [[PubMed](#)]

Sample Availability: Aloin is available from the authors.



© 2018 by the authors. Licensee MDPI, Basel, Switzerland. This article is an open access article distributed under the terms and conditions of the Creative Commons Attribution (CC BY) license (<http://creativecommons.org/licenses/by/4.0/>).